5-29-2013

Biomedical Photoacoustic Imaging Using Gas-coupled Laser Acoustic Detection

Jami L. Johnson
Boise State University

Biomedical Photoacoustic Imaging using Gas-coupled Laser Acoustic Detection

Jami Johnson*
Boise State University
Mechanical and Biomedical Engineering Department
College of Engineering
Faculty Mentors: Michelle Sabick and Kasper van Wijk
(Dated: May 29, 2013)

Abstract: Several detection methods have been explored for photoacoustic and ultrasound imaging of biological tissues. Piezoelectric transducers are commonly used, which require contact with the sample and have limiting bandwidth characteristics. Interferometry detection exhibits improved bandwidth characteristics and resolution, yet generally require complicated optics and the incorporation of a contacting reflective medium. Here, we report the use of a noncontact photoacoustic and laser-ultrasound imaging system that does not require the use of a reflective layer. A simple, robust technique known as gas-coupled laser acoustic detection is used, which has previously been applied to composite material evaluation. This technique has the potential to reduce complexity and cost of photoacoustic imaging devices and allow for use in a broad range of medical applications.

Keywords: photoacoustic imaging, photoacoustic tomography, noncontact, gas-coupled laser acoustic detector, ultrasound, laser-ultrasound, vascular imaging

Introduction

Photoacoustic (PA) imaging is an absorption based imaging modality that utilizes laser-generated ultrasound [1]. The photoacoustic effect begins with a short pulse of laser light that rapidly diffuses when incident on highly scattering biological tissue. The energy of the diffuse beam is absorbed by chromophores in tissue, resulting in transient thermoelastic expansion and generation of acoustic waves. These waves are detected at the surface of the tissue at multiple locations, generating a spatial map of the optical absorbers [2]. Consequently, PA imaging achieves both the high resolution of ultrasound along with high-spectroscopic contrast of optical modalities [3].

Hemoglobin absorbs light in the red to near-infrared spectrum up to six orders of magnitude higher than surrounding tissues [4], lending PA imaging to be particularly well-suited for viewing the structure and function of blood vessels [5]. In addition, molecules such as lipids, water, and melanin have unique absorption spectra that can be exploited by PA imaging [3].

Absorption of laser light at the surface of tissue also generates an acoustic wave, termed the laser-ultrasound (LU) wave. Through careful analysis of LU propagation and scattering, an ultrasound image can be reconstructed. The mechanical information obtained from an LU image compliments PA imaging for a more comprehensive characterization of tissue. Noncontact photoacoustic and laser-ultrasound images were obtained by Rousseau *et al.* [6, 7]. Additionally, we recently applied earth image processing methods to biomedical PA and LU images, described in [8].

The potential for incorporating photoacoustic imaging capabilities into traditional ultrasound systems may be realized using piezoelectric transducers [9, 10]. However, the development of new detecttors for PA and LU imaging is of great interest for several reasons. First, while high sensitivity can be achieved with transducers, they are known to have narrow bandwidths due to the resonant behavior of piezoelectric elements. This limits the size and depth of structures detectable with a given transducer [11]. Additionally, unlike traditional ultrasound modalities, photoacoustic imaging requires illumination of the sample with an optical source beam. Most piezoelectric transducers are made from opaque, ceramic materials. This complicates light delivery when both excitation and detection must be accomplished on one side of the sample. The sensitivity of piezoelectric elements is also limiting for PA and LU applications because sensitivity decreases with element size [12]. Most photoacoustic reconstruction algorithms assume the detector elements are smaller than the structures to be imaged. Achieving adequate resolution and sen-

sitivity for the smallest structures, therefore, is problematic with piezoelectric transducers [12]. Finally, transducers require contact with the sample, making them inappropriate for clinical and surgical procedures where access to the sample is required or applied pressure may cause discomfort or harm.

Several remote detection methods have been developed for photoacoustic imaging applications. Optical interferometers offer advantages over contacting transducers, including broadband frequency characteristics and point-like detection spot sizes [13]. High-resolution photoacoustic images have been achieved using these detectors [11, 14–19], however, limitations remain. In general, interferometers rely on reflections of a probe beam from the sample surface. Consequently, rough or poorly reflecting surfaces, such as skin, require a reflective medium to be incorporated. Noncontact interferometric detection (without the need for a reflective medium) has been accomplished by Rousseau *et al.* [6, 7], using a confocal Fabry-Perot interferometer (CFPI). A high-energy probe beam was pulsed in order to increase sensitivity without exceeding the American National Standard Institute energy exposure limits. Likewise, a two-wave mixing interferometer (TWMI) was successfully used as a photoacoustic detector by Hochreiner *et al.* [20] without a coupling medium. Both CFPI and TWMI interferometers require complicated optics, and obtaining adequate sensitivity while remaining below national standards for energy exposure is a significant design challenge. Fabry-Perot polymer film sensors have been developed for PA imaging as well. These detectors are relatively simple in configuration when compared to traditional interferometers and have high sensitivity across a broad range of frequencies [12, 21]. The polymer film head must be in contact with the sample, however, limiting the scope of medical applications.

Gas-coupled laser acoustic detection (GCLAD) was originally developed for materials evaluation, but possesses advantageous qualities for biomedical imaging. GCLAD overcomes many of the limitations of both transducer and optical detection methods by exploiting the changes in air density that occur when an acoustic wave radiates into air. After propagating through tissue, surface motion causes an arriving PA or LU wave to radiate into the surrounding air, varying the index of refraction [22]. GCLAD measures these small variations by measuring the displacement and deflection signal of a probe beam propagating perpendicular to the wave.

A comparatively simple set-up is used for GCLAD, where a laser beam is directed perpendicular to the direction of wave propagation. A wave changes the index of refraction of the air such that the path of this probe beam is altered. A combination of deflection and displacement of the beam occurs, which is detected with a position sensitive photodetector [22, 23]. The probe beam is never in contact with the tissue, making measurements independent of surface roughness or optical reflectivity [22]. The setup is simple in comparison to interferometers and virtually no realignment is required after initial setup. Additional advantages include broadband frequency detection (determined by the detector electronics), point-like detection spot size in the dimension perpendicular to the beam, and straightforward delivery of the source beam when only one side of the sample is available. GCLAD has been used to record acoustic waves for non-destructive evaluation of solid materials, such as metals, composite materials, and thin films. Imaging of both curved and angle surfaces has also been accomplished by modifying the optical layout to match the surface contour of the sample [24]. To date, GCLAD research has focused on rigid material evaluation, however, the optically rough nature of human skin makes photoacoustic and laser-ultrasound imaging an especially appropriate application for GCLAD. Here, we present the first B-scan images of a tissue phantom using GCLAD as part of a noncontact, robust, and relatively simple imaging system.

Methodology

The experimental set-up is shown in Fig. 1. A solid phantom composed of 1% Intralipid®, 1% highly purified agar (A0930-05, USBiological), and deionized water was used to represent biological soft tissue. Intralipid® phantoms are well studied as tissue-mimicking phantoms for photoacoustic imaging applications, with optical scattering and acoustic properties similar to biological tissues [25–29]. A thin-walled polyester tube (1.57 mm diameter, 12.7 μm wall-thickness) filled with infrared absorbing dye (Epolight™ 2057) was embedded 14 mm below the surface of the phantom. The tube wall was considered acoustically transparent for the wavelength of the source, such that contribution of the tube to PA generation or LU scattering could be neglected.

An unfocused 1064 nm Nd:YAG laser with an 8 mm beam diameter, 10 ns pulse width and repetition rate of 11 Hz was used as the excitation source. A low-noise, 532 nm laser was projected parallel to the phantom surface, passing through a convex lens with a 75 mm focal length. The focused beam was incident on a position-sensitive
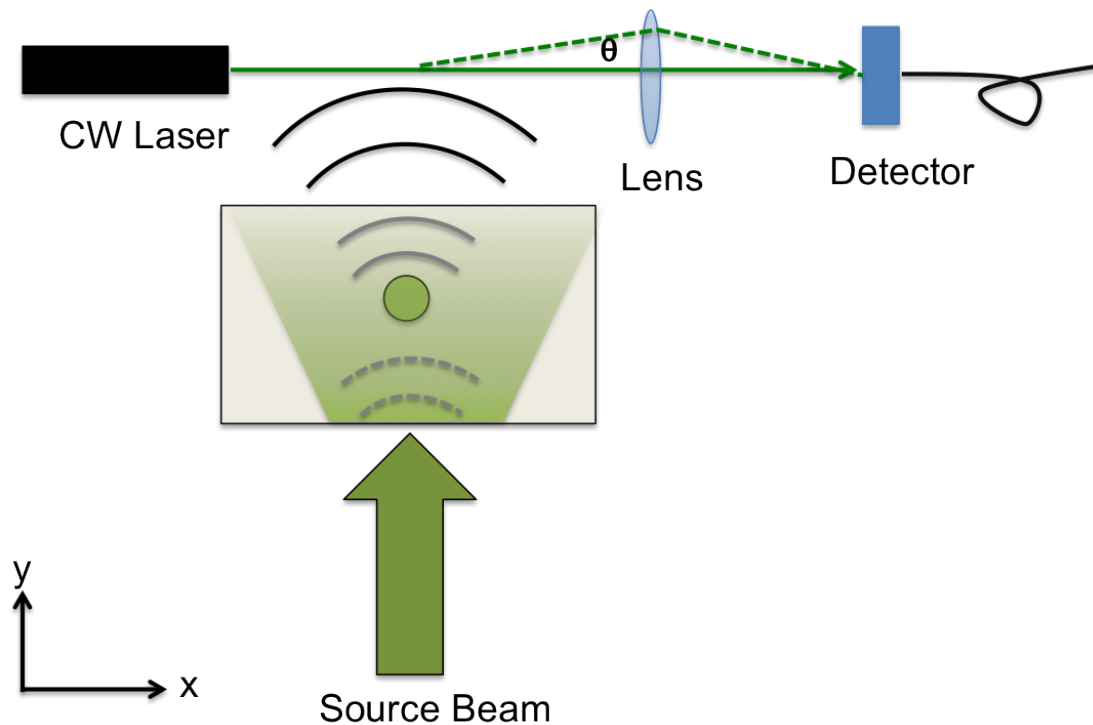
FIG. 1: Setup for photoacoustic transmission experiment with GCLAD. The LU wave generated at the surface of the phantom and PA wave generated by dye in the polyester tube are shown. Both waves propagate through the air and displace the GCLAD probe beam, which is measured by a position-sensitive photodetector.

photodetector (Dulcian, Quarktet) with a frequency bandwidth from 50 kHz to 6 MHz. An air gap of 11 mm lay between the probe beam and the sample surface.

Two-dimensional images were constructed by scanning the phantom in the horizontal (x) direction, Fig. 1. The source and detector remained stationary as the phantom was translated by 0.254 mm increments, covering a scan distance of 19.05 mm. The average of 64 A-scans was recorded at each point, which combined to form a two-dimensional B-scan image. Two trials were recorded, which differed in the energy of the source beam. First, a high energy beam was used that significantly exceeded the maximum permissible exposure (MPE) for a pulsed laser source [30]. Then, the energy of the source beam was reduced to about 100 mJ/cm^2 for the second trial. Further energy analysis will be required to ensure the energy exposure of the source beam is kept below MPE standards for multiple pulses at 1064 nm.

Results

The B-scan images for each trial are shown in Fig. 2. As expected, higher PA and LU amplitudes were observed in the high energy trial, however, excellent signal-to-noise was shown for each image, Fig. 3. As expected, the amplitude of the PA wave decreased with distance from the tube. In each trial, the LU wave amplitude remained relatively constant because the distance between the source and detector remained unchanged throughout the scan.

Interferometers detect acoustic waves directly at the phantom surface. Comparatively, waves detected with GCLAD are delayed due to the additional time required for waves to propagate through air to reach the probe beam. The distance between the phantom surface and detector remained constant and the speed of sound in air is known, therefore, the additional travel time can be easily removed for accurate reconstruction and depth profiling.
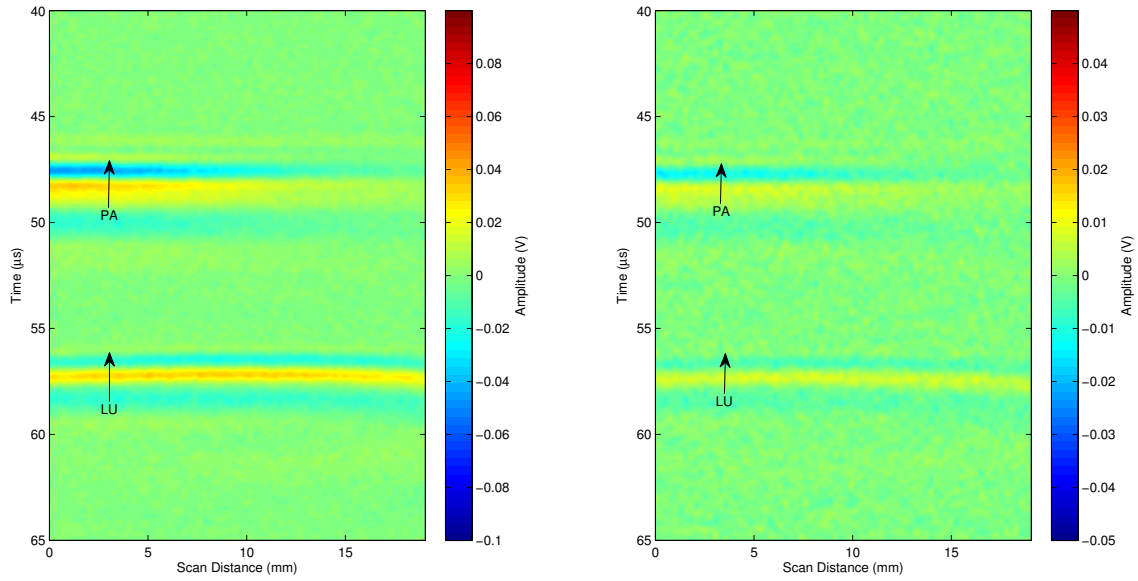
FIG. 2: B-scan images using high energy (left) and low energy (right) source beam.
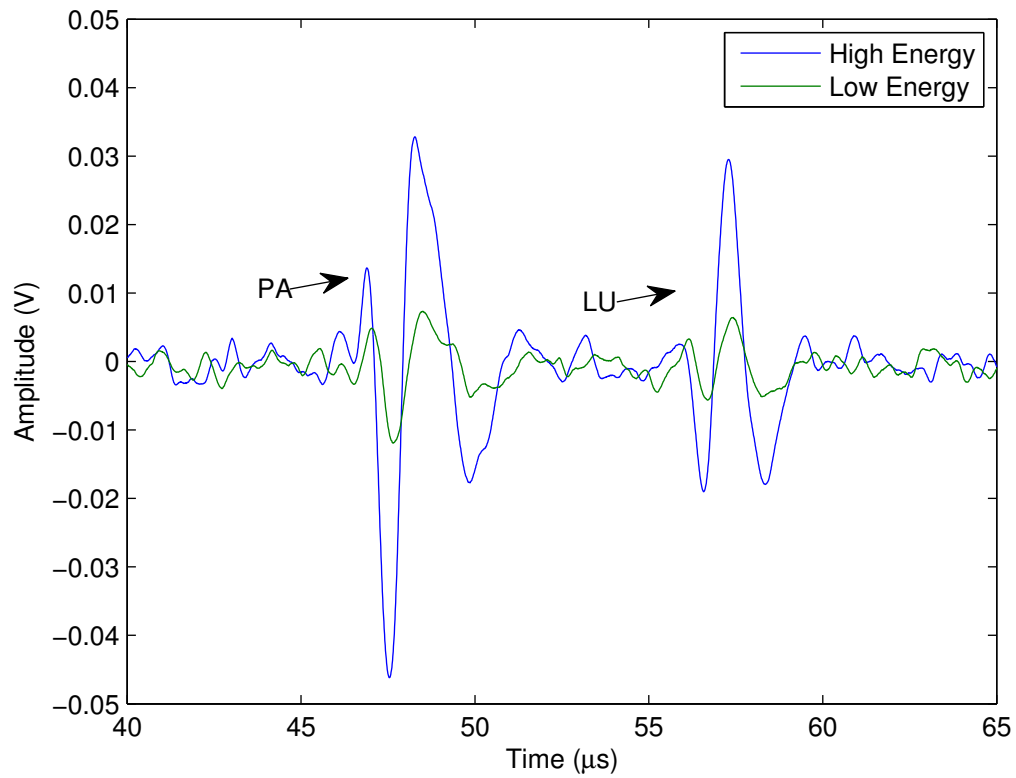
FIG. 3: A-scans of phantom with embedded tube and dye for varying source energy. Both PA and LU waves are shown.

Conclusions

In conclusion, we have shown the feasibility of gas-coupled laser acoustic detection for photoacoustic and laser-ultrasound imaging. Exceptional signal-to-noise was demonstrated with the probe beam a distance greater than 1 cm from the phantom surface. This detector does not require acoustic or optical contact with the sample, eliminating energy exposure concerns for the detector. Noncontact detection has the potential to increase the range of medical applications of laser-generated imaging modalities while reducing cost, complexity, and size.

Acknowledgements

References

* Boise State University, Boise ID, 83725; Electronic address: `jamijohnson1@u.boisestate.edu`

[1] M. Xu and L. Wang. Photoacoustic imaging in biomedicine. *Review of Scientific Instruments*, 77:041101, 2006.

[2] S. Sethuraman, S. Aglyamov, J. Amirian, R. Smalling, and S. Emelianov. Intravascular photoacoustic imaging to detect and differentiate atherosclerotic plaques. *IEEE Ultrasonics Symposium*, 1:133–136, 2005.

[3] J. Beard. Biomedical photoacoustic imaging. *Interface Focus*, 1:602–631, 2011.

[4] Z. Guo, S. Hu, and L. V. Wang. Calibration-free absolute quantification of optical absorption coefficients using acoustic spectra in 3d photoacoustic microscopy of biological tissue. *Optics Letters*, 35(12):2067–2069, 2010.

[5] L. V. Wang and S. Hu. Photoacoustic tomography: In vivo imaging from organelles to organs. *Science*, 335:1458–1462, 2012.

[6] G. Rousseau, B. Gauthier, A. B. Louin, and J.P. Monchalin. Non-contact biomedical photoacoustic and ultrasound imaging. *Journal of Biomedical Optics*, 17(6):061217:1–7, 2012.

[7] G. Rousseau, A. Blouin, and J.P. Monchalin. Non-contact photoacoustic tomography and ultrasonography for tissue imaging. *Biomedical Optics Express*, 3(1):16–25, 2012.

[8] Jami Johnson. Toward characterization of diseased vascular structures using noncontact photoacoustic and laser-ultrasound imaging: A phantom study. Master's thesis, Boise State University, 2013.

[9] C. Kim, T. N. Erpelding, L. Jankovic, and L. V. Wang. Performance benchmarks of an array-based hand-held photoacoustic probe adapted from a clinical ultrasound system for non-invasive sentinel lymph node imaging. *Philosophical Transactions of The Royal Society*, 369:4644–4650, 2011.

[10] C. Kim, T. N. Erpelding, L. Jankovic, M. D. Pashley, and L. V. Wang. Deeply penetrating in vivo photoacoustic imaging using a clinical ultrasound array system. *Biomedical Optics Express*, 1(1):278–284, 2010.

[11] G. Paltauf, R. Nuster, M. Haltmeier, and P. Burgholzer. Photoacoustic tomography using a mach-zehnder interferometer as an acoustic line detector. *Applied Optics*, 46(16):3352–3358, 2007.

[12] E. Zhang, J. Laufer, and P. Beard. Backward-mode multiwavelength photoacoustic scanner using a planar fabry-perot polymer film ultrasound sensor for high-resolution three-dimensional imaging of biological tissues. *Applied Optics*, 47(4):561–577, 2008.

[13] H. Kihm, S. A. Carp, and V. Venugopalan. *Interferometry-Based Optoacoustic Tomography*. CRC Press, 2009.

[14] B. P. Payne, V. Venugopalan, B. B. Mimić, and N. S. Nishioka. Optoacoustic tomography using time-resolved interferometric detection of surface displacement. *Journal of Biomedical Optics*, 8(2):273–280, 2003.

[15] S. A. Carp, A. Guerra, S. Q. Duque, and V. Venugopalan. Optoacoustic imaging using interferometric measurement of surface displacement. *Applied Physics Letters*, 85(23):5772–5774, 2004.

[16] G. Paltauf, R. Nuster, M. Haltmeier, and P. Burgholzer. Experimental evaluation of reconstruction algorithms for limited view photoacoustic tomography with line detectors. *Inverse Problems*, 23:S81–S94, 2007.

[17] M. Holotta, H. Grossauer, C. Kremser, P. Torbica, J. Völkl, G. Degenhart, R. Esterhammer, R. Nuster, G. Paltauf, and W. Jaschke. Photoacoustic tomography of *ex vivo* mouse hearts with myocardial infarction. *Journal of Biomedical Optics*, 16(3):036007, 2011.

[18] R. Nuster, S. Gratt, K. Passler, D. Meyer, and G. Paltauf. Photoacoustic section imaging using an elliptical acoustic mirror and optical detection. *Journal of Biomedical Optics*, 17(3):030503, 2012.

[19] Y. Wang, C. Li, and R. K. Wang. Noncontact photoacoustic imaging achieved by using a low-coherence interferometer as the acoustic detector. *Optics Letters*, 36(20):3975–3977, 2011.

[20] A. Hochreiner, T. Berer, H. Grün, M. Leitner, and P. Burgholzer. Photoacoustic imaging using an adaptive interferometer with a photorefractive crystal. *Journal of Biophotonics*, 5(7):508–517, 2012.

[21] E. Z. Zhang and P. Beard. 2d backward-mode photoacoustic imaging system for nir (650-1200nm) spectroscopic biomedical applications. In *Proceedings of SPIE*, volume 6086, page 6086H, 2006.

[22] J. N. Caron, Y. Yang, and J. B. Mehl. Gas-coupled laser acoustic detection at ultrasonic and audio frequencies. *Review of Scientific Instruments*, 69(8):2912–2917, 1998.

[23] J. N. Caron. Displacement and deflection of an optical beam by airborne ultrasound. *Review of Progress in Quantitative Nondestructive Evaluation*, 27A:247, 2008.

[24] J. N. Caron, K. V. Steiner, Y. Yang, and J. B. Mehl. Gas coupled laser acoustic detection for ultrasound inspection of composite materials. *Materials Evaluation*, 58(5):667–671, 2000.

[25] L. Yao, Y. Sun, and H. Jiang. Transport-based quantitative photoacoustic tomography: simulations and experiments. *Physics in Medicine and Biology*, 55:1917–1934, 2010.

[26] S. T. Flock, S. L. Jacques, B. C. Wilson, W. M. Star, and M. J. C. van Gemert. Optical properties of intralipid: A phantom medium for light propagation studies. *Lasers in Surgery and Medicine*, 12:510–519, 1992.

[27] M. Kinnunen and R. Myllylä. Effect of glucose on photoacoustic signals at the wavelengths of 1064 nm and 532 nm in pig blood and intralipid. *Journal of Physics D: Applied Physics*, 38:2654–2661, 2005.

[28] I. Driver, J. W. Feather, P. R. King, and J. B. Dawson. The optical properties of aqueous suspensions of intralipid, a fat emulsion. *Physics in Medicine and Biology*, 34(12):1927–1930, 1989.

[29] R. Cubeddu, A. Pifferi, P. Taroni, A. Torricelli, and G. Valentini. A solid tissue phantom for photon migration studies. *Physics in Medicine and Biology*, 42:1971–1979, 1997.

[30] *American National Standard for Safe Use of Lasers*. Number Z136.1. Laser Institute of America, 2007.